HHS Public Access

Author manuscript

J Phys Chem B. Author manuscript; available in PMC 2016 September 03.

Published in final edited form as:

J Phys Chem B. 2015 September 3; 119(35): 11618–11625. doi:10.1021/acs.jpcb.5b06536.

Toward Relatively General and Accurate Quantum Chemical Predictions of Solid-State ^{17}O NMR Chemical Shifts in Various Biologically Relevant Oxygen-containing Compounds

Amber Rorick, **Matthew A. Michael**, **Liu Yang**, and **Yong Zhang***

Department of Chemistry, Chemical Biology and Biomedical Engineering, Stevens Institute of Technology, 1 Castle Point on Hudson, Hoboken NJ 07030, USA

Abstract

Oxygen is an important element in most biologically significant molecules and experimental solid-state ^{17}O NMR studies have provided numerous useful structural probes to study these systems. However, computational predictions of solid-state ^{17}O NMR chemical shift tensor properties are still challenging in many cases and in particular each of the prior computational work is basically limited to one type of oxygen-containing systems. This work provides the first systematic study of the effects of geometry refinement, method and basis sets for metal and non-metal elements in both geometry optimization and NMR property calculations of some biologically relevant oxygen-containing compounds with a good variety of XO bonding groups, X= H, C, N, P, and metal. The experimental range studied is of 1455 ppm, a major part of the reported ^{17}O NMR chemical shifts in organic and organometallic compounds. A number of computational factors towards relatively general and accurate predictions of ^{17}O NMR chemical shifts were studied to provide helpful and detailed suggestions for future work. For the studied various kinds of oxygen-containing compounds, the best computational approach results in a theory-versus-experiment correlation coefficient R^2 of 0.9880 and mean absolute deviation of 13 ppm (1.9% of the experimental range) for isotropic NMR shifts and R^2 of 0.9926 for all shift tensor properties. These results shall facilitate future computational studies of ^{17}O NMR chemical shifts in many biologically relevant systems, and the high accuracy may also help refinement and determination of active-site structures of some oxygen-containing substrate bound proteins.

Introduction

Oxygen is an important element found in most biologically significant molecules such as proteins, nucleic acids, carbohydrates, and phospholipids. It is also at the center of numerous biological processes. Among the four most common biological elements: oxygen, hydrogen, carbon and nitrogen, oxygen is the element that only has a quadrupolar NMR-active stable isotope, ^{17}O. This isotope is unique because its spin state is 5/2 as opposed to the 1/2 spin state seen in most frequently used isotopes of the other three elements**.** ^{17}O has a natural

Phone: +1-201-216-5513, yong.zhang@stevens.edu.

Supporting Information Available

The methodological studies of ~60 method combinations for the ^{17}O NMR chemical shift tensor properties of compound **6** are available free of charge via the Internet at http://pubs.acs.org.

abundance of only 0.037%,[1-4] which makes solid-state ^{17}O NMR studies rather challenging. However, recent experimental techniques have dramatically advanced this field and a number of types of oxygen-containing systems have been experimentally investigated,[1-4] including various kinds of biologically relevant systems, such as those with CO,[5, 6] NO,[7, 8] and PO[9] groups, amino acids,[10-13] nucleic acid bases,[14] pharmaceutical compounds,[15] and large protein-ligand complexes.[16] More recently, the solid-state ^{17}O NMR studies have even been extended to some paramagnetic metal complexes with organic ligands.[17]

To help understand experimental solid-state ^{17}O NMR results, a number of theoretical investigations have been reported, such as those on the calculated ^{17}O NMR shifts of amides[5], nucleic acid bases[14, 18-20], amino acids[11-13], carboxylic compounds[21-23], peptides[24] as well as a few metal containing compounds[7, 8, 17, 25]. For the diamagnetic systems, regarding the two major types of solid-state ^{17}O NMR properties, the ^{17}O NMR chemical shielding/shift tensor and electric field gradient tensor (or related quadrupole coupling constant), previous results show that quantum chemical predictions of the latter one are in most cases satisfactory with errors <10%, while the accurate predictions of the former one are relatively more challenging. For instance, in the case of amide compounds, previous work show that the mean percentage deviation (MPD) of the predicted ^{17}O NMR isotropic chemical shifts (δiso's) is about twice of the MPD of the calculated ^{17}O quadrupole coupling constants.[5] The predictions of δiso's though in some cases can achieve an accuracy of <10-15% error, but also frequently have errors well above 20-30%, especially for metal-containing systems.[5, 7-9, 11-14, 17-25]

Clearly more studies are needed in order to make more accurate predictions of ^{17}O NMR chemical shifts in diamagnetic oxygen-containing systems, which can also help future investigations of the diamagnetic contributions of the ^{17}O NMR chemical shifts in paramagnetic oxygen-containing species. In addition, each of the published computational studies of ^{17}O NMR chemical shifts is basically focused on one type of chemical systems. Therefore, this work aims to provide a relatively general computational approach towards accurate predictions of ^{17}O NMR chemical shifts in a good variety of biologically relevant diamagnetic oxygen-containing systems, including HO, CO, NO, PO, and MO (M = metal) bonding groups. In addition, this work provides a systematic investigation of the computational factors on ^{17}O NMR chemical shift predictions, including geometry, method of choice, basis scheme for both non-metal and metal elements, which points out some useful factors for future computational work of other oxygen-containing species. Results show that the overall calculated ^{17}O NMR chemical shift tensor principal elements (δ_{11}'s, δ_{22}'s, δ_{33}'s) in an experimental range of 1455 ppm have an excellent theory-versus-experiment correlation coefficient R^2=0.9926, and the mean absolute deviation (MAD) of the predicted δiso's is 13 ppm, with 5.7% MPD. These results shall help future computational studies of ^{17}O NMR chemical shifts, which may also help structure refinement of some substrate bound proteins[16] as done previously by using quantum chemical studies of other NMR chemical shifts.[26, 27]

Computational Details

The structures studied in this work are shown in Figure 1: (**1**) oxalic acid[23], (**2**) chloromaleic acid[21], (**3**) triphenylphosphine oxide[28], (**4**) L-valine[13], (**5**) *p*-nitrosodimethylaniline (NODMA) hydrochloride hydrate[8, 29] , (**6**) $SnCl_2(CH_3)_2(NODMA)_2$[8] and (**7**) Fe(TPP)(1-methylimidazole)(CO)[25], TPP = tetraphenylporphyrinato (here the phenyl substituent is replaced by hydrogen). These molecules contain a good variety of bonding groups 'XO' where X= H, C, N, P, and Sn. A number of factors that could affect the accuracy of ^{17}O NMR chemical shift predictions were studied, including geometry, method of choice, basis schemes for both non-metal and metal elements. All calculations were done using *Gaussian 09*.[30]

Regarding geometry, both the original X-ray crystal structures of these molecules and partial geometry optimization with ~60 density functional theory (DFT) methods and basis set combinations were investigated, see details in the next section. Since previous work has repeatedly highlighted the importance of the inclusion of hydrogen bonding partners in ^{17}O NMR chemical shift predictions,[6, 11, 14] here by default, the hydrogen bonding partners are included in the calculations for compounds **1**, **2**, **4**, as shown in Figure 1. In this work, only the first shell of hydrogen bonding partners of the nuclei of interest were studied since our goal is to develop an efficient computational approach for future studies of large biologically relevant molecules and the current results have already been of excellent theory-versus-experiment correlations with systematic errors that can be reduced by using predictions from regression results (*vide infra*).

Regarding NMR chemical shielding calculations, the gauge independent atomic orbital (GIAO) algorithm used in previous computational studies[5-8, 14, 25] was also employed here. Both the pure DFT method OP86[31, 32] and the hybrid DFT method B3LYP[33] together with Pople-type basis 6-311++G(d,p) and 6-311++G(2d,2p), and Dunning type basis D95(d,p)[34] and aug-cc-PVDZ[35] for non-metal elements and the effective core potential basis LanL2DZ[36] for metals were studied. Based on our recent work on some oxygen-containing systems[17] and more studies in the Supporting Information, the LanL2DZ basis yields the best NMR shift predictions among a number of metal bases studied. Although the state-of-the-art CCSD(T) calculations shall provide better predictions of absolute NMR shift values than DFT methods,[37] their uses are basically limited to small molecules. Therefore, to help develop a computational approach to study biologically relevant large molecules, we focused on the investigation of DFT calculations here.

The calculated chemical shielding tensor elements (σ_{ij}) were then converted to the chemical shifts tensor elements (δ_{ij}) using the standard ^{17}O reference H_2O. The formula $\delta = 287.5 - \sigma$ was used in order to obtain calculated chemical shift results, in which 287.5 ppm is the experimental absolute chemical shielding for liquid water,[38] which is also similar to a more recent determination from high resolution rotational spectroscopy,[39] 289.2 ppm.

Results and Discussion

In this first work to have a systematic investigation of the effects of the used geometry, method, basis sets of both non-metal and metal elements towards a relatively general

computational approach for accurate predictions of ^{17}O NMR chemical shifts in some biologically relevant systems, a number of oxygen-containing compounds as shown in Figure 1 were chosen as a representative date set for those with HO, CO, NO, PO, and MO bonding patterns. Their experimental ^{17}O NMR chemical shift tensor principal elements or isotropic shifts are listed in Table 1, which contain 22 independent data points covering an experimental range of 1455 ppm, a major part of the reported ^{17}O NMR chemical shifts in organic and organometallic compounds.[1]

Oxalic acid was the first model investigated here. As shown in Figure 1, based on the X-ray crystal structure,[23] each oxalic acid molecule is surrounded by six hydrogen bonded water molecules. Since previous work has repeatedly highlighted the importance of the inclusion of hydrogen bonding partners in ^{17}O NMR chemical shift predictions,[6, 11, 14] this model with all six surrounding water molecules was used, which was previously found to have only 3.7% deviation regarding the largest and most affected tensor element from the use of a much more sophisticated and time-consuming model of 11 oxalic acid and 29 water molecules.[23] We first tested the use of the X-ray structure without any geometry optimization. Although previously the quantum chemical methods at both the Hartree-Fock and DFT levels[5, 7-9, 11, 13-17, 19, 21, 23-25, 28] were used for NMR chemical shielding calculations, here we focused on evaluating DFT methods, since eventually we will also investigate metal-containing systems. Both the pure DFT method OP86[31, 32] and the hybrid DFT method B3LYP[33] were studied here based on their previous good performance in predicting ^{17}O NMR chemical shifts in some limited sets of oxygen-containing compounds.[8, 13, 17, 19, 21, 23, 24] Regarding the basis sets, the relatively large Dunning type basis D95(d,p)[34] and aug-cc-PVDZ[35] and Pople-type basis 6-311++G(d,p) were investigated based on previous studies.[8, 13, 19, 21-25] The calculated ^{17}O NMR chemical shift tensor principal elements and isotropic shifts are shown in Table 2, along with the linear correlation coefficients and slopes for the regression of the calculated ^{17}O NMR chemical shift tensor principal elements vs. experimental values. As shown in Table 2, both OP86 and B3LYP for each basis set tested have excellent predictions since R^2 are all basically larger than 0.990, which is consistent with their excellent performance reported previously.[8, 13, 17, 19, 21, 23, 24] OP86 results here have slightly better R^2 than B3LYP data for all the studied basis sets. The average deviation of the slopes from ideal values is 6.7% for B3LYP calculations and 2.6% for OP86 calculations, again showing slightly better performance of OP86. For each method, the differences in R^2 from using a different basis set are also small (<0.0025). However, the differences in slopes are a little bit larger. Based on the results in Table 2, the method combination of OP86/6-311++G(d,p) has the best R^2 (0.9943) and slope (1.0187) values.

Next, partial geometry optimization calculations were run on the same X-ray structure for **1** with only the hydrogen atoms being optimized. Here we focused on the evaluation of the effect of the hydrogen positions, since they are basically uncertain in conventional X-ray structures, and the above calculations using the X-ray structure have already yielded excellent results, which do not necessitate the use of more extensive geometry refinement. Due to the excellent performance of OP86 method in the above study, it was also examined as a method for geometry optimization, along with a modest size basis set 6-31G(d), which may be applied to relatively large systems to help future work on biologically relevant

systems. Interestingly, as shown in Table 3, the geometry optimization on hydrogen positions indeed results in improvement in both R^2 and slope, and this improvement occurs for both NMR calculations methods OP86 and B3LYP. Here, the use of a larger basis set of 6-311++G(2d,2p) compared to 6-311++G(d,p) yields almost the same R^2 values and <1% difference in slopes. The best NMR computational method combination appears again to be OP86/6-311++G(d,p), with R^2=0.9967 and slope=1.0059. In addition, another geometry optimization method based on the studies on metal-containing systems (*vide infra*), mPWP86/6-311G(d), was also investigated here. Results in Table 3 show that this method also generates similarly excellent calculations, with R^2's and slopes slightly inferior to those obtained using the OP86/6-31G(d) optimized structure.

Overall, these results show that both the pure DFT and hybrid DFT methods can yield excellent predictions of the ^{17}O NMR chemical shift tensor properties for this relatively simple system. In addition, data here also support the use of refined geometries, consistent with many prior reports which employed partial refinement of hydrogen positions,[6, 14] and in some more difficult cases the refinement of other key group (e.g. MNO)[7], and the whole crystal structure experimentally[8] or computationally.[9, 15] Therefore, the partial geometry optimization with only hydrogen positions refined was used in subsequent calculations.

Three more molecules (**2-4**) were then examined in order to see the excellent accuracy in the calculated ^{17}O NMR chemical shifts for **1** could be extended to a few more organic molecules with either a different XO bonding group (PO in **3**) or different intermolecular interactions and substituents around CO groups (**2**, **4**), see Figure 1. The computed ^{17}O NMR properties are shown in Table 4. As seen from Table 5 regarding the associated statistical analysis data for compounds **1-4**, the overall accuracy is still excellent since R^2 values are all above 0.984. With more data included in the regression analysis, now the computed ^{17}O NMR properties from using B3LYP are of slightly better correlation with experiment than those from using OP86, though the slopes of B3LYP NMR calculations are still of larger deviations from the ideal value. The larger slopes results in slightly increased MAD's by 2-3 ppm in the case of using OP86/6-31G(d) optimized structures. Regarding the basis set effect, now results from using 6-311++(2d,2p) are of marginally better correlations and better slopes, see Table 5. The use of another geometry optimization method mPWP86/6-311G(d) again results in similar and marginally less accurate data compared to the geometry optimization method OP86/6-31(d), with R^2 values decreased by ≤ 0.0018. Here, the best MAD is only 3.1% of the experimental shift range (481 ppm) for compounds **1-4**.

After obtaining accurate results for above organic molecules we then investigated the relatively more challenging NO-containing molecules and metal complexes **5-7**.[7, 8] For instance, in the case of **6** containing both NO and metal, the initial calculations using the X-ray structure have errors in δ_{iso} of 171-192 ppm (24-27%), which is similar to the errors of 202-218 ppm (28-30%) reported in the previous work.[8] Therefore, a detailed methodological study on geometry optimization method and basis sets for both non-metal and metal elements as well as NMR property calculation method and basis sets for both non-metal and metal elements using ~60 different method combinations was performed (see details in Supporting Information). The best calculated isotropic shift has an error dramatically

descreased to 45 ppm or 6.3%. As shown in Table 5, after the data of compouds **5-7** are included in the statisitical analysis, the R^2's for NMR calculation method OP86 have been slightly reduced from ~0.98 to ~0.97, and the slopes have clear deterioration (~10-20% worse), indicating that these compounds are more challenging for computational studies. However, the R^2's for NMR calculation method B3LYP are slightly increased to be above 0.992 along with a more moderate deterioration in slopes. These results clearly indicate that 1) the effects of the geometry refinement and the method and basis set choices for metal elements in both geometry optimization and NMR calculations are significant; 2) the hybrid DFT method B3LYP appears to be better than the pure DFT method OP86 in ^{17}O NMR chemical shift tensor property calculations when more challenging compounds are included; 3) the geometry optimization methods OP86/6-31G(d) and mPWP86/6-311G(d) are of similar performance with the latter one having slightly better R^2's, slopes, and MAD's. Overall, considering R^2, slope, and MAD, the best method combination here is to use mPWP86 with QZVP for metals and 6-311G(d) for non-metals in geometry optimization and use B3LYP with LanL2DZ for metals and 6-311++G(2d,2p) for non-metals in NMR calculation. It has an MAD of 36 ppm for all ^{17}O NMR chemical shift tensor properties studied here, which is only 2.5% of the toal experimental range of 1455 ppm. As illustrated in Figure **2**, the calculated chemical shift properties not only have an excellent overall correlation with R^2 of 0.9926, but also basically evenly distributed around the regress line. In addition, as shown in Table 6 for the statistical results for isotropic ^{17}O NMR chemical shifts in all compounds **1**-7, the slope and MAD data are all better than those for the ^{17}O NMR chemical shift tensor property calculations. The best method combination for the isotropic shift calculation is the same as for the tensor property calculations, with R^2 of 0.988 and MAD of 23 ppm, or 3.4% of the experimental isotropic shift range of 672 ppm, see Table 1. The theory-versus-experiment correlation can be seen in Figure **3**, again having all data points well distributed around the regress line to indicate the overall excellent accuracy. Since its slope still has ca. 8% deviation from the ideal value, we further evaluated the use of regression line information to predict isotropic shifts as follows:

$$\delta^{\mathrm{pred}} = \left(\delta^{\mathrm{calc}} + 6.84\right) / 1.0838$$

The data are listed in Table 7 for the best method combination here. Because the shifts predicted using the regression line have ideal slope (1.0000) and intercept (0 ppm) compared to experimental data, the MAD was further reduced to be only 13 ppm, which is just 1.9% of the experimental shift range. The MPD of 5.7% is also excellent.

Conclusions

This work provides the first systematic study of the effects of geometry refinement, method and basis sets for metal and non-metal elements in both geometry optimization and NMR property calculations of some biologically relevant oxygen-containing compounds with a good variety of XO bonding groups, X= H, C, N, P, and M. Results suggest a number of important factors towards relatively general and accurate predictions of ^{17}O NMR chemical shifts.

Geometry optimization is highly recommended, in particular for those containing metal or other special groups (such as NO). The partial geometry optimization involving just hydrogen atoms is essential as they are basically uncertain in conventional X-ray structures, and in more difficult cases, partial geometry optimization of local groups or full crystal structure refinements may be needed to help achieve reasonable accuracy as reported previously.[7-9, 15] The pure DFT methods used here are good for geometry optimization, with mPWP86/6-311(d) being slightly better. For future work on other systems particularly containing other metal centers, the major attention is suggested to be on metal basis selection during the geometry optimization, as this was found out to be most influential on accuracy (e.g. up to ~350 ppm or ~50% error in δ_{iso} of **6**).

Regarding ^{17}O NMR chemical shift tensor property calculations, both the hybrid DFT method B3LYP and the pure DFT method OP86 were found to be good for organic molecules, but when more challenging metal- and NO-containing compounds are included, B3LYP is better. The basis set of 6-311++G(d,p) in this step is sufficient to produce excellent results, with a larger basis set of 6-311++G(2d,2p) having slightly better performance.

Overall, the best method combination based on above systematic investigation of a number of different types of biologically relevant oxygen-containing chemical systems is to use mPWP86 with the QZVP basis for metals and 6-311G(d) basis for non-metals in geometry optimization and use B3LYP with LanL2DZ for metals and 6-311++G(2d,2p) for non-metals in NMR calculation. It has an excellent R^2 of 0.9926, with an MAD of 36 ppm for all ^{17}O NMR chemical shift tensor properties studied here, being only 2.5% of the toal experimental range of 1455 ppm. The predictions of the isotropic NMR shifts are also excellent, with R^2 of 0.988 and MAD of only 13 ppm, which is just 1.9% of the experimental shift range. These results shall facilitate future computational studies of ^{17}O NMR chemical shifts in various biologically relevant systems, and the high accuracy may also help structure refinement and determination of some substrate bound proteins as done previously.[26, 27]

Supplementary Material

Refer to Web version on PubMed Central for supplementary material.

Acknowledgement

This work was supported by an NIH grant GM085774 to YZ.

References

(1). Wu G. Solid-state ^{17}O NMR Studies of Organic and Biological Molecules. Prog. Nucl. Magn. Res. Spectr. 2008; 52:118–169.

(2). Lemaitre V, Smith ME, Watts A. A Review of Oxygen-17 Solid-State NMR of Organic Materials--Towards Biological Applications. Solid State Nucl. Magn. Reson. 2004; 26:215–235. [PubMed: 15388187]

(3). Gerothanassis IP. Oxygen-17 NMR Spectroscopy: Basic Principles and Applications (Part II). Prog. Nucl. Magn. Reson. Spectr. 2010; 57:1–110.

(4). Gerothanassis IP. Oxygen-17 NMR Spectroscopy: Basic Principles and Applications (Part I). Prog. Nucl. Magn. Reson. Spectr. 2010; 56:95–197.

(5). Yamada K, Dong S, Wu G. Solid-state O-17 NMR Investigation of the Carbonyl Oxygen Electric-Field-Gradient Tensor and Chemical Shielding Tensor in Amides. J. Am. Chem. Soc. 2000; 122:11602–11609.

(6). Dong S, Ida R, Wu G. A Combined Experimental and Theoretical 17O NMR Study of Crystalline Urea: An Example of Large Hydrogen-bonding Effects. J. Phys. Chem. A. 2000; 104:11194–11202.

(7). Godbout N, Sanders LK, Salzmann R, Havlin RH, Wojdelski M, Oldfield E. Solid-state NMR, Mossbauer, Crystallographic, and Density Functional Theory Investigation of Fe-O-2 and Fe-O-2 Analogue Metalloporphyrins and Metalloproteins. J. Am. Chem. Soc. 1999; 121:3829–3844.

(8). Wu G, Zhu J, Mo X, Wang R, Terskikh V. Solid-state (17)O NMR and Computational Studies of C-nitrosoarene Compounds. J. Am. Chem. Soc. 2010; 132:5143–5155. [PubMed: 20307099]

(9). Gervais C, Profeta M, Lafond V, Bonhomme C, Azais T, Mutin H, Pickard CJ, Mauri F, Babonneau F. Combined Ab initio Ccomputational and Experimental Multinuclear Solid-state Magnetic Resonance Study of Phenylphosphonic Acid. Magn. Reson. Chem. 2004, 42, 445–452.

(10). Pike KJ, Lwmaitre V, Kukol A, Anupold T, Samson A, Howes AP, Watts A, Smith ME, Dupree R. Solid-State 17O NMR of Amino Acids. J. Phys. Chem. B. 2004; 108:9256–9263.

(11). Gervais C, Dupree R, Pike KJ, Bonhomme C, Profeta M, Pickard CJ, Mauri F. Combined First-Principles Computational and Experimental Multinuclear Solid-State NMR Investigation of Amino Acids. J. Phys. Chem. A. 2005; 109:6960–6969. [PubMed: 16834055]

(12). Yamada K, Honda H, Yamazaki T, Yoshida M. Solid-state 17O NMR Study of the Electric-Field-Gradient and Chemical Shielding Tensors in Polycrystalline Gamma-Glycine. Solid State Nucl. Magn. Reson. 2006; 30:162–170. [PubMed: 17045787]

(13). Yamada K, Nemoto T, Asanuma M, Honda H, Yamazaki T, Hirota H. Both Experimental and Theoretical Investigations of Solid-state 17O NMR for L-valine and L-isoleucine. Solid State Nucl. Magn. Reson. 2006; 30:182–191. [PubMed: 17074470]

(14). Wu G, Dong S, Ida R, Reen N. A Solid-State O-17 Nuclear Magnetic Resonance Study of Nucleic Acid Bases. J. Am. Chem. Soc. 2002; 124:1768–1777. [PubMed: 11853455]

(15). Kong X, Shan M, Terskikh V, Hung I, Gan Z, Wu G. Solid-State 17O NMR of Pharmaceutical Compounds: Salicylic Acid and Aspirin. J. Phys. Chem. B. 2013; 117:9643–9654. [PubMed: 23879687]

(16). Zhu JF, Ye E, Terskikh V, Wu G. Solid-state ^{17}O NMR Spectroscopy of Large Protein-Ligand Complexes. Angew. Chem.-Int. Edit. 2010; 49:8399–8402.

(17). Kong X, Terskikh V, Khade RL, Yang L, Rorick A, Zhang Y, He P, Huang Y, Wu G. Solid-State 17O NMR Spectroscopy of Paramagnetic Coordination Compounds. Angew. Chem.-Int. Ed. 2015; 54:4753–4757.

(18). Ida R, De Clerk M, Wu G. Influence of N-H…O and C-H…O Hydrogen Bonds on the ^{17}O NMR Tensors in Crystalline Uracil: Computational Study. J. Phys. Chem. A. 2006; 110:1065–1071. [PubMed: 16420009]

(19). Amini SK, Shaghaghi H, Bain AD, Chabok A, Tafazzoli M. Magnetic Resonance Tensors In Uracil: Calculation of ^{13}C, ^{15}N, ^{17}O NMR Chemical Shifts, ^{17}O and ^{14}N Electric Field Gradients and Measurement of ^{13}C and ^{15}N Chemical Shifts. Solid State Nucl. Magn. Reson. 2010; 37:13–20. [PubMed: 20071154]

(20). Kwan IC, Mo X, Wu G. Probing Hydrogen Bonding and Ion-Carbonyl Interactions by Solid-state ^{17}O NMR Spectroscopy: G-ribbon and G-quartet. J. Am. Chem. Soc. 2007; 129:2398–407. [PubMed: 17269776]

(21). Wong A, Pike KJ, Jenkins R, Clarkson GJ, Anupold T, Howes AP, Crout DH, Samoson A, Dupree R, Smith ME. Experimental and Theoretical ^{17}O NMR Study of the Influence of Hydrogen-bonding on C=O and O-H Oxygens in Carboxylic Solids. J. Phys. Chem. A. 2006; 110:1824–1835. [PubMed: 16451014]

(22). Wu G, Yamada K. Determination of the ^{17}O NMR Tensors in Potassium Hydrogen Dibenzoate: A Salt Containing a Short O…H…O Hydrogen Bond. Solid State Nucl. Magn. Reson. 2003; 24:196–208. [PubMed: 12943914]

(23). Zhang Q, Chekmenev EY, Wittebort RJ. ^{17}O Quadrupole Coupling and Chemical Shielding Tensors in an H-Bonded Carboxyl Group: Alpha-Oxalic Acid. J. Am. Chem. Soc. 2003; 125:9140–9146. [PubMed: 15369371]

(24). Chekmenev EY, Waddell KW, Hu J, Gan Z, Wittebort RJ, Cross TA. Ion-Binding Study by ^{17}O Solid-State NMR Spectroscopy in the Model Peptide Gly-Gly-Gly at 19.6 T. J. Am. Chem. Soc. 2006; 128:9849–9855. [PubMed: 16866542]

(25). Salzmann R, Ziegler CJ, Godbout N, McMahon MT, Suslick KS, Oldfield E. Carbonyl Complexes of Iron(II), Ruthenium(II), and Osmium(II) 5,10,15,20-Tetraphenylporphyrinates: A Comparative Investigation by X-Ray Crystallography, Solid-State NMR Spectroscopy, and Density Functional Theory. J. Am. Chem. Soc. 1998; 120:11323–11334.

(26). Mao JH, Mukherjee S, Zhang Y, Cao R, Sanders JM, Song YC, Zhang YH, Meints GA, Gao YG, Mukkamala D, Hudock MP, Oldfield E. Solid-State NMR, Crystallographic, and Computational Investigation of Bisphosphonates and Farnesyl Diphosphate Synthase-Bisphosphonate Complexes. J. Am. Chem. Soc. 2006; 128:14485–14497. [PubMed: 17090032]

(27). Yang L, Ling Y, Zhang Y. HNO Binding in a Heme Protein: Structures, Spectroscopic Properties, and Stabilities. J. Am. Chem. Soc. 2011; 133:13814–13817. [PubMed: 21834502]

(28). Bryce DL, Eichele K, Wasylishen RE. An ^{17}O NMR and Quantum Chemical Study of Monoclinic and Orthorhombic Polymorphs of Triphenylphosphine Oxide. Inorg. Chem. 2003; 42:5085–96. [PubMed: 12924879]

(29). Drangfelt O, Romming C. Crystal Structure of N,N-Dimethyl-p-nitrosoaniline Hydrochloride Hydrate. Acta Chem. Scand. 1974; 28:1101–1105.

(30). Frisch, MJ.; Trucks, GW.; Schlegel, HB.; Scuseria, GE.; Robb, MA.; Cheeseman, JR.; Scalmani, G.; Barone, V.; Mennucci, B.; Petersson, GA., et al. Gaussian, Inc.; Wallingford CT: 2010. Gaussian 09, Revision B.01

(31). Hoe W-M, Cohen A, Handy NC. Assessment of a New Local Exchange Functional OPTX. Chem. Phys. Lett. 2001; 341:319–328.

(32). Perdew JP. Density-functional Approximation for the Correlation Energy of the Inhomogeneous Electron Gas. Phys. Rev. B. 1986; 33:8822–8824.

(33). Becke AD. Density-Functional Thermochemistry .3. the Role of Exact Exchange. J. Chem. Phys. 1993; 98:5648–5652.

(34). Dunning, TH, Jr. In Modern Theoretical Chemistry. Schaefer, HF., III, editor. Vol. 3. Plenum; New York: 1977. p. 1-28.

(35). Davidson ER. Comment on ‘Comment on Dunning's correlation-consistent basis sets’. Chem. Phys. Lett. 1996; 260:541–518.

(36). Hay PJ, Wadt WR. Ab initio Effective Core Potentials for Molecular Calculations. Potentials for the Transition Metal Atoms Scandium to Mercury. J. Chem. Phys. 1985; 82:270–283.

(37). Teale AM, Lutnas OB, Helgaker T, Tozer DJ, Gauss J. Benchmarking Density-functional Theory Calculations of NMR Shielding Constants and Spin–Rotation Constants Using Accurate Coupled-Cluster Calculations. J. Chem. Phys. 2013; 138:024111. [PubMed: 23320672]

(38). Wasylishen RE, Bryce DL. A Revised Experimental Absolute Magnetic Shielding Scale for Oxygen. J. Chem. Phys. 2002; 117:10061–10066.

(39). Puzzarini C, Cazzoli G, Harding ME, Vázquez J, Gauss J. A New Experimental Absolute Nuclear Magnetic Shielding Scale for Oxygen Based on the Rotational Hyperfine Structure of H_2O^{17}. J. Chem. Phys. 2009; 131:234304. [PubMed: 20025326]

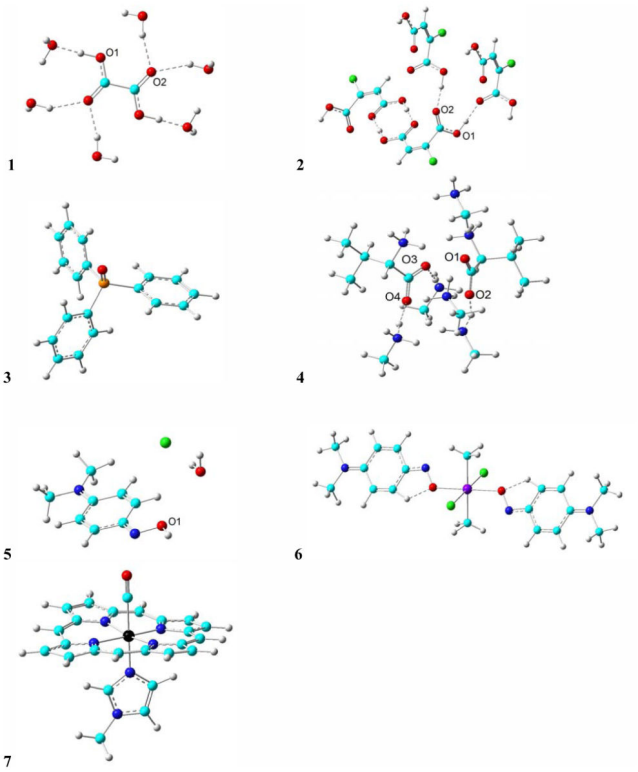

Figure 1.

Structures of the molecules (**1**-**7**) investigated in this work. Atom color scheme: Cl – green; O – red; P – orange; C – cyan; H – gray; N – blue; Fe – black; Tin – violet. Single dashed lines indicate hydrogen bonds. Where there are multiple oxygens, the labeled ones are with NMR properties studied.

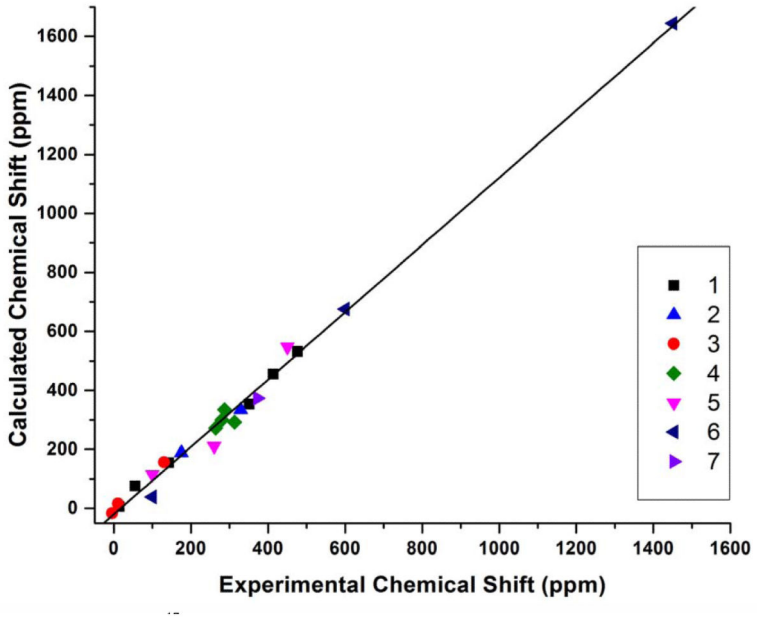

Figure 2.

Calculated ^{17}O NMR chemical shift tensor properties from using the mPWP86/6-311G(d) geometry optimization and B3LYP/6-311++G(2d,2p) NMR calculation vs. experimental data for compounds **1-7**.

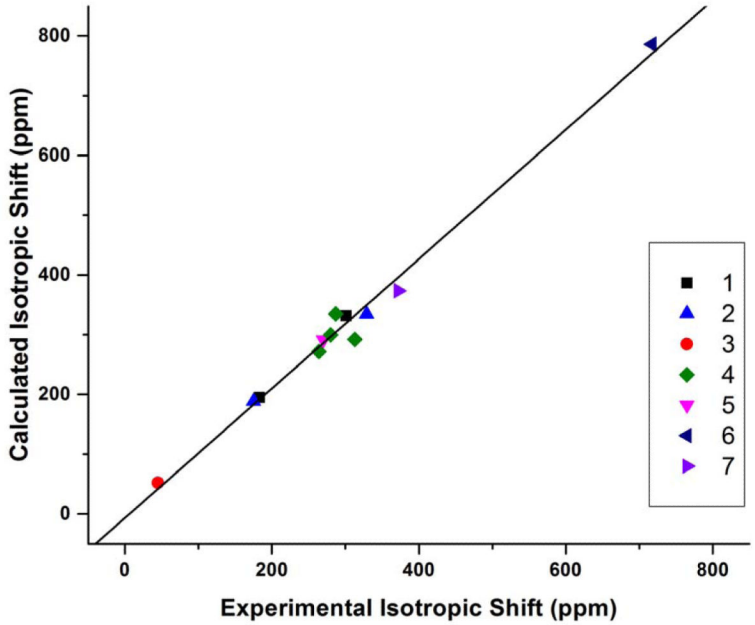

Figure 3.

Calculated ^{17}O NMR isotropic chemical shifts from using the mPWP86/6-311G(d) geometry optimization and B3LYP/6-311++G(2d,2p) NMR calculation vs. experimental data for compounds **1-7**.

Table 1

Experimental ^{17}O NMR chemical shifts (unit: ppm)

System	Atom		Value	Reference
1	O1	δ_{11}	351	23
		δ_{22}	142	
		δ_{33}	55	
		δ_{iso}	183	
	O2	δ_{11}	476	
		δ_{22}	413	
		δ_{33}	14	
		δ_{iso}	301	
2	O1	δ_{iso}	175	21
	O2	δ_{iso}	329	
3	O	δ_{11}	130	28
		δ_{22}	11	
		δ_{33}	−5	
		δ_{iso}	45	
4	O1	δ_{iso}	313	13
	O2	δ_{iso}	280	
	O3	δ_{iso}	264	
	O4	δ_{iso}	287	
5	O1	δ_{11}	450	8, 29
		δ_{22}	260	
		δ_{33}	100	
		δ_{iso}	270	
6	O	δ_{11}	1450	8
		δ_{22}	600	
		δ_{33}	100	
		δ_{iso}	717	
7	O	δ_{iso}	372	25

Table 2

Calculated ^{17}O NMR Data from using the X-Ray Structure of **1** (unit: ppm)

Method	Basis Set		δ_{11}	δ_{22}	δ_{33}	δ_{iso}	R^2	Slope
B3LYP	aug-cc-pVDZ	O1	309	126	59	165	0.9895	1.0261
		O2	493	421	−1	304		
	6-311++G(d,p)	O1	345	144	75	188	0.9911	1.0925
		O2	535	458	10	334		
	D95(d,p)	O1	328	135	57	173	0.9919	1.0825
		O2	509	447	−6	317		
OP86	aug-cc-pVDZ	O1	303	133	59	165	0.9920	0.9748
		O2	466	408	−1	292		
	6-311++G(d,p)	O1	334	148	73	185	0.9943	1.0187
		O2	497	434	10	314		
	D95(d,p)	O1	324	145	56	175	0.9932	1.0339
		O2	483	435	−6	304		

Table 3

Calculated ^{17}O NMR Data for the Partially Optimized Structure of **1** (unit: ppm)

Optimization	NMR		δ_{11}	δ_{22}	δ_{33}	δ_{iso}	R^2	Slope
OP86/ 6-31G(d)	B3LYP/ 6-311++G(d,p)	O1	362	156	77	198	0.9965	1.0783
		O2	521	454	6	327		
	B3LYP/ 6-311++G(2d,2p)	O1	360	156	76	197	0.9964	1.0762
		O2	522	451	7	327		
	OP86/ 6-311++G(d,p)	O1	349	160	74	194	0.9967	1.0059
		O2	484	431	6	307		
	OP86/ 6-311++G(2d,2p)	O1	347	160	73	194	0.9967	1.0070
		O2	486	429	6	307		
mPWP86/ 6-311G(d)	B3LYP/ 6-311++G(d,p)	O1	354	155	77	195	0.9938	1.0933
		O2	532	460	6	332		
	B3LYP/ 6-311++G(2d,2p)	O1	353	155	76	195	0.9937	1.0889
		O2	532	456	6	331		
	OP86/ 6-311++G(d,p)	O1	342	159	74	192	0.9951	1.0189
		O2	494	435	5	311		
	OP86/ 6-311++G(2d,2p)	O1	341	160	74	192	0.9951	1.0177
		O2	495	433	6	311		

Table 4

Calculated ^{17}O NMR Data for the Partially Optimized Structures of **2-7** (unit: ppm)

Optimization	Compound	Property	NMR: OP86 6-311++G(d,p)	6-311++G(2d,2p)	NMR: B3LYP 6-311++G(d,p)	6-311++G(2d,2p)
OP86/6-31G(d)	**2**	O1 δ_{iso}	187	186	189	188
		O2 δ_{iso}	319	319	336	335
	3	O1 δ_{11}	166	166	157	156
		O1 δ_{22}	9	14	7	16
		O1 δ_{33}	−20	−20	−22	−16
	4	O1 δ_{iso}	280	279	293	293
		O2 δ_{iso}	280	280	294	293
		O3 δ_{iso}	260	260	271	271
		O4 δ_{iso}	320	319	337	335
	5	O1 δ_{11}	734	705	551	545
		O1 δ_{22}	222	223	213	214
		O1 δ_{33}	109	107	114	112
	6	O δ_{11}	1743	1761	1735	1743
		O δ_{22}	632	635	692	695
		O δ_{33}	40	40	41	41
	7	O δ_{iso}	336	335	374	374
mPWP86/6-311G(d)	**2**	O1 δ_{iso}	187	179	181	189
		O2 δ_{iso}	319	349	372	335
	3	O1 δ_{11}	166	166	157	156
		O1 δ_{22}	9	14	7	16
		O1 δ_{33}	−21	−20	−22	−16
	4	O1 δ_{iso}	279	279	293	292
		O2 δ_{iso}	286	286	300	299
		O3 δ_{iso}	261	261	272	272
		O4 δ_{iso}	320	318	336	335
	5	O1 δ_{11}	734	706	554	548
		O1 δ_{22}	220	221	211	211
		O1 δ_{33}	112	110	117	115
	6	O δ_{11}	1632	1650	1634	1644
		O δ_{22}	614	617	672	676
		O δ_{33}	39	37	39	39
	7	O δ_{iso}	336	335	374	374

Table 5

Statistical Analysis Results for ^{17}O NMR Chemical Shift Tensor Properties

Compounds	Optimization	NMR	R^2	Slope	MAD
1-4	OP86/6-31G(d)	OP86/6-311++G(d,p)	0.9857	1.0021	15
		OP86/6-311++G(2d,2p)	0.9860	0.9982	15
		B3LYP/6-311++G(d,p)	0.9883	1.0718	18
		B3LYP/6-311++G(2d,2p)	0.9885	1.0597	17
	mPWP86/6-311G(d)	OP86/6-311++G(d,p)	0.9848	1.0111	16
		OP86/6-311++G(2d,2p)	0.9859	1.0171	16
		B3LYP/6-311++G(d,p)	0.9870	1.0954	22
		B3LYP/6-311++G(2d,2p)	0.9867	1.0687	18
1-7	OP86/6-31G(d)	OP86/6-311++G(d,p)	0.9705	1.2011	44
		OP86/6-311++G(2d,2p)	0.9745	1.2094	44
		B3LYP/6-311++G(d,p)	0.9924	1.1985	41
		B3LYP/6-311++G(2d,2p)	0.9921	1.2012	40
	mPWP86/6-311G(d)	OP86/6-311++G(d,p)	0.9683	1.1340	40
		OP86/6-311++G(2d,2p)	0.9737	1.1433	39
		B3LYP/6-311++G(d,p)	0.9926	1.1386	38
		B3LYP/6-311++G(2d,2p)	0.9926	1.1412	36

Table 6

Statistical Analysis Results for ^{17}O NMR Isotropic Shifts in Compounds **1-7**

Optimization	NMR	R^2	Slope	MAD
OP86/6-31G(d)	OP86/6-311++G(d,p)	0.9590	1.0977	26
	OP86/6-311++G(2d,2p)	0.9619	1.1076	26
	B3LYP/6-311++G(d,p)	0.9855	1.1424	26
	B3LYP/6-311++G(2d,2p)	0.9846	1.1448	26
mPWP86/6-311G(d)	OP86/6-311++G(d,p)	0.9616	1.0316	23
	OP86/6-311++G(2d,2p)	0.9674	1.0482	23
	B3LYP/6-311++G(d,p)	0.9880	1.0892	26
	B3LYP/6-311++G(2d,2p)	0.9880	1.0838	23

Table 7

Predicted ^{17}O NMR Isotropic Shifts from Using the Best Approach

Compound	Atom	δ^{pred}	$\lvert\Delta\delta^{pred}\rvert$ *a)*	$\lvert\Delta\delta^{pred}\rvert$ %
1	O1	186	3	1.7%
	O2	312	11	3.7%
2	O1	180	5	3.0%
	O2	315	14	4.3%
3	O	54	9	20.6%
4	O1	276	37	11.9%
	O2	283	3	0.9%
	O3	257	7	2.7%
	O4	315	28	9.8%
5	O1	275	5	1.9%
6	O	732	15	2.0%
7	O	351	21	5.7%
Average			13	5.7%

a) This is the absolute deviation from experiment.